AAS 15-202

USING ONBOARD TELEMETRY FOR MAVEN ORBIT DETERMINATION

Drew Jones[*], Try Lam[†], Nikolas Trawny[‡], and Clifford Lee[§]

Determining the state of Mars orbiting spacecraft has traditionally been achieved using radiometric tracking data, often with data before and after an atmospheric drag pass. This paper describes our approach and results for supplementing radiometric observables with on-board telemetry measurements to improve the reconstructed trajectory estimate for the Mars Atmosphere and Volatile Evolution Mission (MAVEN). Uncertainties in Mars atmospheric models, combined with non-continuous tracking degrade navigation accuracy, making MAVEN a key candidate for using on-board telemetry data to help complement its orbit determination process. The successful demonstration of using telemetry data to improve the accuracy of ground based orbit determination could reduce cost (DSN tracking time) and enhance the performance of future NASA missions. In addition, it presents an important stepping stone to autonomous on-board aerobraking and aerocapture.

INTRODUCTION

THE Mars Atmosphere and Volatile Evolution Mission (MAVEN), part of NASA's Mars Scout program, was launched on November 18, 2013 and will explore the planet's upper atmosphere and its interaction with the Sun and solar wind. During the mission's science phase, the spacecraft will spend approximately 1 year orbiting Mars in an elliptical orbit with a period of 4.5 hours. During each periapsis pass, at altitudes between 125 to 150 km, the drag force from Mars's atmosphere will produce a change in MAVEN's velocity (Δv).

MAVEN differs from previous Mars aerobraking missions in many aspects, such as orbital period, available tracking data, and requirements. Although MAVEN will not be aerobraking, it will encounter drag Δv at periapses much greater than that of Mars Reconnaisaince Orbiter (MRO) science orbit (but significantly less than that of MRO's aerobraking orbits). The nominal MAVEN science orbit will have drag Δv of a few millimeters (3-9 mm/s) per second per orbit, with a varying periapsis altitude designed to maintain a density between 0.05 and 0.15 kg/km^3. The science phase will also include five so-called deep dips, during which periapsis altitude is reduced to achieve densities between 2 and 3.5 kg/km^3. During deep dips the drag effect may be more than 10 times greater (80-180 mm/s) than during the nominal science orbit. Unfortunately, MAVEN's periapsis altitude

[*]Jet Propulsion Laboratory, California Institute of Technology, M/S 264-282, 4800 Oak Grove Dr., Pasadena, CA 91109, 818.354.2056, drew.r.jones@jpl.nasa.gov.

[†]Jet Propulsion Laboratory, California Institute of Technology, M/S 264-820, 4800 Oak Grove Dr., Pasadena, CA 91109, 818.354.6901, try.lam@jpl.nasa.gov.

[‡]Jet Propulsion Laboratory, California Institute of Technology, M/S 198-235, 4800 Oak Grove Dr., Pasadena, CA 91109, 818.343.8685, nikolas.trawny@jpl.nasa.gov.

[§]Jet Propulsion Laboratory, California Institute of Technology, M/S 230-104, 4800 Oak Grove Dr., Pasadena, CA 91109, 818.343.8685, clifford.lee@jpl.nasa.gov.

and orbit inclination of 75 degrees are sufficiently different from previous Mars missions such that little data exists to characterize atmospheric density in this regime. Outside of the deep-dip phases, MAVEN will only have one 7-hour DSN Doppler tracking pass per day (two 5-hour HGA 2-way Doppler passes and five 7-hour LGA 2-way Doppler passes per week). With an orbit period of 4.5 hours this results in 1 out of 5 orbits having full tracking data coverage, which is in stark contrast to previous Mars aerobraking missions, which maintained continuous Doppler coverage.

Maven motivation for using Telemetry Observables in Orbit Determination

Two critical Orbit Determination (OD) requirements during the science phase are (1) the uncertainty in the predicted time of periapsis passage is to be no more than 20 seconds, and (2) the uncertainty in the reconstructed position is to be no more than 3 km (3-σ). For the nominal tracking scenario of one tracking pass per day, the expected reconstruction uncertainty meets the 3 km requirement; however, there exist worst-case contingency scenarios where requirements cannot be satisfied. Atmospheric density is the driving error source for Maven, and orbit-to-orbit density scale factor changes of 100% are anticipated. Accurate reconstruction of daily-weekly density trends, despite the large short-term variability, is vital to reliably predict the density, and therefore maintain the required nominal science corridor of 0.05 and 0.15 kg/km^3. The predict model will utilize current mean density estimates, but unlike other Mars missions there may only be 1-2 recent density reconstructions to use. Furthermore, the spacecraft will alternate its orientation as it goes through the drag pass (switching between maximum and minimum drag area) which can cause inconsistencies in the density estimates. Figure 1 shows the spacecraft in its nominal science-phase configuration, with the boresight of the high gain antenna (HGA) is along the +Z axis and the fixed solar panels are along the +/-Y axes.

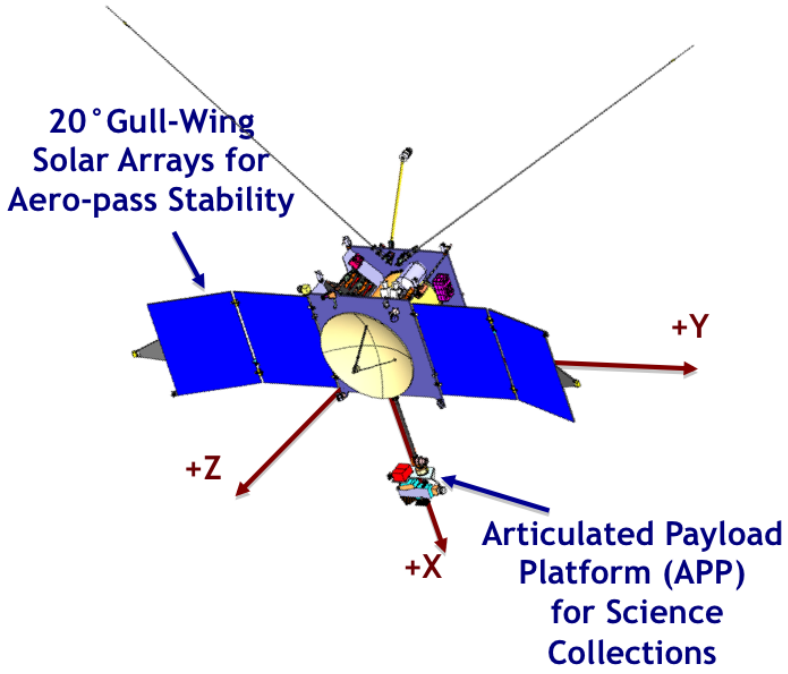

Figure 1. MAVEN spacecraft in its nominal science-phase configuration.

An added complication is that momentum dumps are scheduled to occur near every periapsis, such that their resulting Δv is difficult to differentiate from atmospheric drag Δv (let alone the majority of passes which occur without radiometric tracking). This introduces greater uncertainty in atmospheric density, and therefore degrades estimated density and ephemeris accuracies. In summary, error sources within current Mars atmospheric models, combined with non-continuous deep space network (DSN) tracking, make MAVEN a key candidate to use on-board telemetry data to complement its orbit determination process.[1]

MAVEN already relies on IMU data in the form of its Periapse Timing Estimator (PTE), which takes IMU data as truth to predict subsequent periapsis passage times.[2] PTE does not involve filtering nor integration of the trajectory, and is not used for navigation nor for controlling the density corridor. It is expected that the use of on-board telemetry data (accelerometer and reaction wheel speeds) as OD observables may improve the accuracy of MAVEN's orbit reconstruction and prediction, when included as part of a filtered batch estimation.

JPL motivation for using Telemetry Observables in Orbit Determination

On-board telemetry has recently received growing interest for use in applications such as atmosphere reconstruction and autonomous aerobraking (e.g. Tolson et al,[3] Jah et al.,[4] and O'Shaughnessy et al.[5]). It is readily apparent that the use of telemetry derived observables would be useful during thruster calibration activities, as well as in modeling various non-gravitational accelerations with higher fidelity. Such data is already used by spacecraft subsystem teams during thruster calibrations, but Jah et al.[4] were the first to formulate the use of the IMU observable for reconstructing spacecraft trajectories (specifically during aerobraking). This work combines telemetry derived observables with radiometric data in a batch OD filter, for a non-aerobraking spacecraft mission. This paper describes an approach and preliminary results for supplementing radiometric observables with on-board telemetry measurements to improve the reconstructed trajectory estimate and subsequent trajectory prediction. Thereby, this Maven specific effort, is intended to also represent a general extension of the batch OD software, MONTE,[6] currently in use and developed at the Jet Propulsion Laboratory (JPL).

MODELS AND ESTIMATION

Mars Atmosphere Model

Navigation is using the Mars-GRAM 2005 (MG05) Mars atmosphere model.[7] In the baseline orbit determination process, a scale factor to the MG05 model is the estimated parameter to obtain the corrected density (the parameter scales with the drag Δv). MRO navigation data exhibits significant short and long term variations in the MG05 scale factor, and this is also expected for Maven. Figure 2 shows 3-day averaged (39-orbits) density scale factor estimates for different Mars-GRAM variants during MRO's primary science phase. MRO data also shows very large variations in the the density scale factor for all latitude (almost 100% around the mean near the equator), as shown in Figure 3.

MAVEN expects drag conditions between those of MRO aerobraking and MRO science phases. MAVEN's periapsis latitude will oscillate around the equator (+/-78 degrees), and will spend a majority of the time near +/-40 degrees latitude, where MRO saw large density variations. After MRO's aerobraking phase its periapsis remained near the same latitude, whereas MAVEN's periapsis latitude may change as much as 2.5 degrees in 3 days. The true atmosphere of Mars (and therefore the

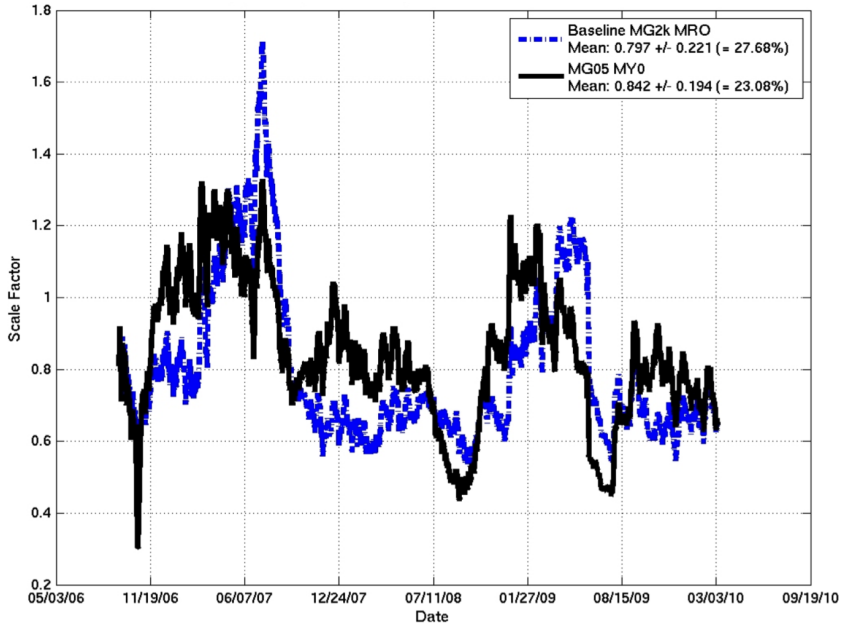

Figure 2. MRO 3-day effective atmospheric drag scale-factor.

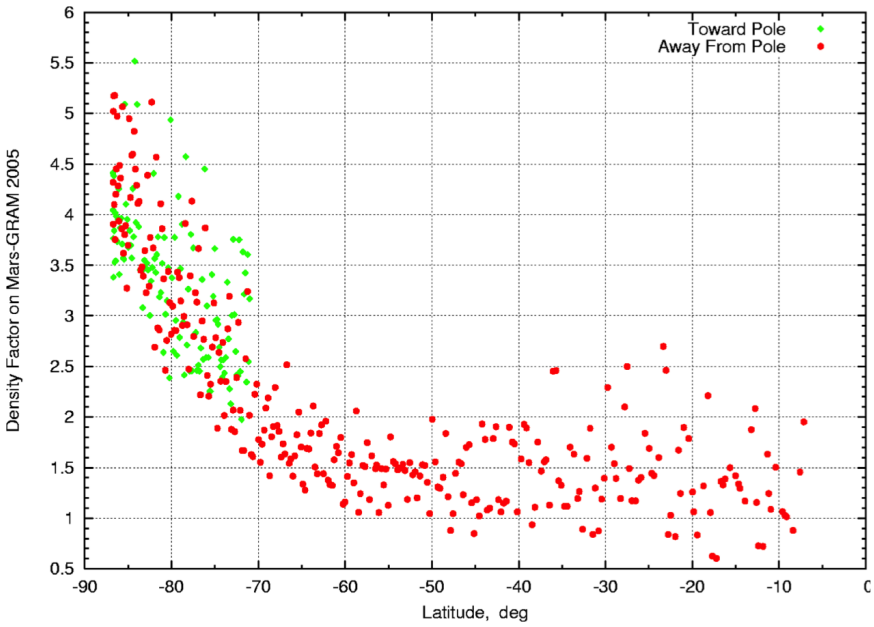

Figure 3. MRO Aerobraking atmospheric drag scale-factor as function of latitude.

density scale factor) is highly dependent on latitude, and therefore those uncertain variations will further degrade the MAVEN navigation team's trajectory predictions. Lastly, unlike MRO which was sun-synchronous, MAVEN's obit will go through large variations in its Sun-relative orientation. Based on all of the above observations, MAVEN navigation is assuming a mean density scale factor 3-σ uncertainty of 50% (1-day average), but orbit-to-orbit uncertainties of 100% (3-σ).

MONTE

MONTE is the current orbit determination software used at JPL.[6] The general form of MONTE's discrete-time Kalman filter can be found in Bierman.[8] The estimated parameter vector can be separated into four categories: state, bias, stochastic, and consider parameters. The state and bias parameters covariance can be influenced by the state transition matrix time updates, but are not influenced by any noise or stochastic. Stochastics are parameters that can change over a time internal due to a discrete noise process, and can be applied to discrete time batches. Consider parameters have uncertainties that are in the estimation process but are not estimated. Furthermore, estimated parameters may be constrained, such that their nominal apriori value is never updated during subsequent iterations of the filter. The MG05 density scale factor is generally treated as a white-noise stochastic bias, with a batch that spans from apoapsis to apoapsis.

Telemetry Derived Observables

Accelerometer (IMU) Telemetry data used by Navigation are similar to that required by the science team and are provided by the spacecraft team on the telemetry server after a spacecraft downlink. The IMU measures non-gravitational acceleration, and this is available as an acceleration vector $\mathbf{a}_o$ (in the S/C body frame) from raw telemetry. The observed quantity is then

$$a_o = \|\mathbf{a}_o\|$$

A design choice we have made is to process acceleration magnitude instead of the full acceleration vector, since it limits sensitivity to attitude errors, and reduces the number of measurements to process. Primary deterministic accelerometer measurement errors include a scale factor error term and a non-zero bias term.[9] Therefore, the computed accelerometer magnitude is given by the equation

$$a_c = s_a\|\mathbf{a}\| + b_a = s_a\|\mathbf{a}_{\text{total}} - \mathbf{a}_{\text{grav}}\| + b_a \tag{1}$$

where, $\mathbf{a}_{\text{total}}$ is the total acceleration vector of the spacecraft, $\mathbf{a}_{\text{grav}}$ is the total gravitational acceleration vector, s_a is a 1st order scale-factor error and b_a is a bias. It is worth noting that the bias b_a in the acceleration magnitude model, is not equal to the norm of the physical accelerometer bias, since $\|s_a\mathbf{a} + b_a\| <= s_a\|\mathbf{a}\| + \|b_a\|$. Therefore, this bias may change some as a function of the periapsis attitude orientation, but this is considered a second order error source. The bias and scale factor terms are implemented primarily to provide additional tuning parameters, and in the baseline strategy will be inferred initially, and set as constants (will not be estimated parameters).

In addition, a clock offset (bias term) is introduced to account for a shift in the onboard clock (and therefore the time tags associated with the accelerometer measurements). The baseline approach is to infer this measurement time offset during calibrations, rather than estimate it as a parameter, since it should change very slowly (if at all) over the science phase.

Torque from reaction wheel speeds The external torque acting on the spacecraft, $\vec{\tau}$, is the other quantity formulated as an observable (however results utilizing this data are reserved for future work). Unlike the accelerometer observable, the torque observable is not directly available from raw telemetry, and therefore some pre-processing steps are necessary to generate the torque measurements. The observed torque (measurement) is derived from available rotational quantities, including the Reaction Wheel Assembly (RWA), but neglecting the Articulated Payload Platform (APP), as

$$\vec{\tau}_o = \begin{bmatrix} \tau_x \\ \tau_y \\ \tau_z \end{bmatrix} = \dot{\mathbf{H}} = \dot{\mathbf{H}}_{\text{sc}} + \dot{\mathbf{H}}_{\text{rwa}} + \vec{\omega}_{\text{sc}} \times (\mathbf{H}_{\text{sc}} + \mathbf{H}_{\text{rwa}})$$

Where all vectors are assumed in the spacecraft body frame, and defined as

- System angular momentum vector, $\mathbf{H}$.
- Spacecraft bus angular momentum vector, $\mathbf{H}_{\text{sc}}$.
- RWA angular momentum vector, $\mathbf{H}_{\text{rwa}}$.
- Spacecraft angular rate vector, $\vec{\omega}_{\text{sc}}$

The net angular momentum of the RWA, in the body frame, is obtained from the individual wheel speeds (telemetry data) and their respective known rotation matrices. Also, the time-derivatives of $\mathbf{H}_{\text{sc}}$ and $\mathbf{H}_{\text{rwa}}$ are obtained during pre-processing via numerical finite differencing.

Drag Force Model

Most JPL missions compute the atmospheric drag force and the solar radiation pressure force, by decomposing the spacecraft into discrete shape elements, and summing their net effect. The MAVEN baseline strategy instead uses tabulated drag coefficients obtained from a computational fluid dynamics (CFD) simulation. The tabulated coefficients are available at 5-degree increments (ra/dec) of the incoming flow direction. A net atmospheric drag force is typically given as

$$\mathbf{f}_d = -\frac{1}{2}\rho v^2 \left[A\ c_d\right] \hat{v} \tag{2}$$

Where ρ is the density, v the relative speed (with direction $\hat{v}$), A the net drag area, and c_d the net (or effective) coefficient of drag. But with the adopted tabulated CFD approach, the drag force is written as

$$\mathbf{f}_d = -\frac{1}{2}\rho v^2 \left[\bar{c}_d(\hat{v})\right] \hat{v} \tag{3}$$

Where, $\bar{c}_d$ is the quantity interpolated from the table using the spherical angles of $\hat{v}$ as interpolates. Obviously, the computed quantity a_c is dependent on $\mathbf{f}_d$ via Eq. (1), since the drag acceleration is one of the $\mathbf{a}_{\text{total}}$ terms.

The CFD table also provides moment coefficients lending themselves to a drag torque computation. The computed aerodynamic torque using a moment coefficient vector (with components cm_x, cm_y, and cm_z) in the spacecraft body frame is

$$\vec{\tau}_d = -\frac{1}{2}\rho v^2 \begin{bmatrix} cm_x(\hat{v}) \\ cm_y(\hat{v}) \\ cm_z(\hat{v}) \end{bmatrix} \tag{4}$$

However, at this time the MONTE software does not implement the Eq. 4 computation with interpolation of the flow direction $\hat{v}$. Therefore, the use of the external torque observable is not considered in the results of this manuscript, but its inclusion will be presented in a future work. Additionally, $\vec{\tau}_d$ is only one external torque term in the full computed torque, and other factors include SRP torque and torque from finite burns. These additional effects must be considered for high fidelity results.

Estimated Parameters

In general, partial derivatives of the a_c observable with respect to various non-gravitational force parameters are available. Within the scope of this paper, the following parameters are considered observable via the accelerometer measurements, and may be estimated

- Atmospheric drag (ρ or MG05 density scale factor)
- Finite burn direction and magnitude (Δv or thrust magnitude)
- Finite burn start/end times (equivalently start time and burn duration)
- Empirical (3-axis polynomial) acceleration (to indirectly model general non-gravitational perturbations)

For MAVEN, the atmospheric density scale factor is of particular interest, and telemetry (in conjunction with radiometric data) should prove valuable in separating drag Δv from momentum desaturation (desat) Δv, during visible passes. Furthermore, during reconstruction of periapsis passes lacking radiometric tracking, telemetry observables provide the only information about density for those orbits. The MG05 density scale factor is generally estimated as a stochastic bias, updated at each apoapsis.The empirical acceleration provides much flexibility, as it may be modeled as a polynomial function over some duration, as small/short independent segments of constant acceleration, or using a stochastic batches with some correlation over some duration.

RESULTS

In preparation for Maven science phase, this methodology was calibrated using MAVEN cruise data, during trajectory correction maneuvers 1 and 2. This provided the opportunity to establish tools for pre-processing actual MAVEN data. Second, MRO data was used to test and refine the setup and procedures for MAVEN in the nominal science phase, including its use to estimate density scale factors over consecutive drag passes. These calibration results better represent the unique challenges of a Mars orbiting phase (as opposed to cruise phase). Lastly, actual Maven science data is utilized during the nominal science phase, and for select maneuver reconstructions. The first major application of the method will be undertaken during the first Deep-Dip campaign, scheduled for February 12-18 of 2015.

Cruise phase TCM calibrations

MAVEN TCM-1 occurred on December 3, 2013, and consisted of two finite burns. The first a settling burn involving the TCM thrusters, followed by a main burn on the MOI thrusters. TCM-2 was executed on February 26, 2014, and consisted of a single finite burn involving TCM thrusters. The burns were modeled nominally as constant thrust finite burns of specified start time and duration. For TCM-1, the accelerometer observable exhibited a clear 6-second shift with respect to the

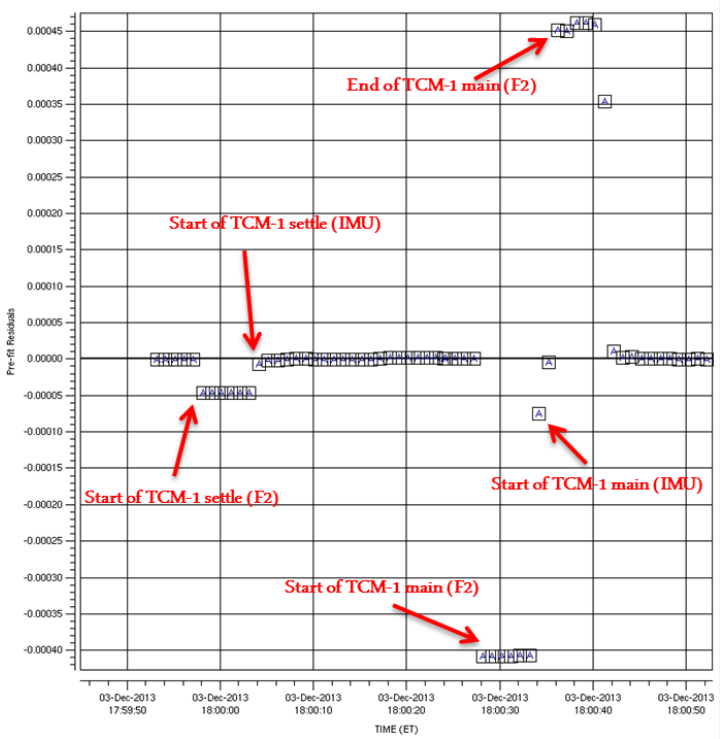

Figure 4. MAVEN Accelerometer Residuals during TCM-1, Annotated to Show Measurement Clock Offset.

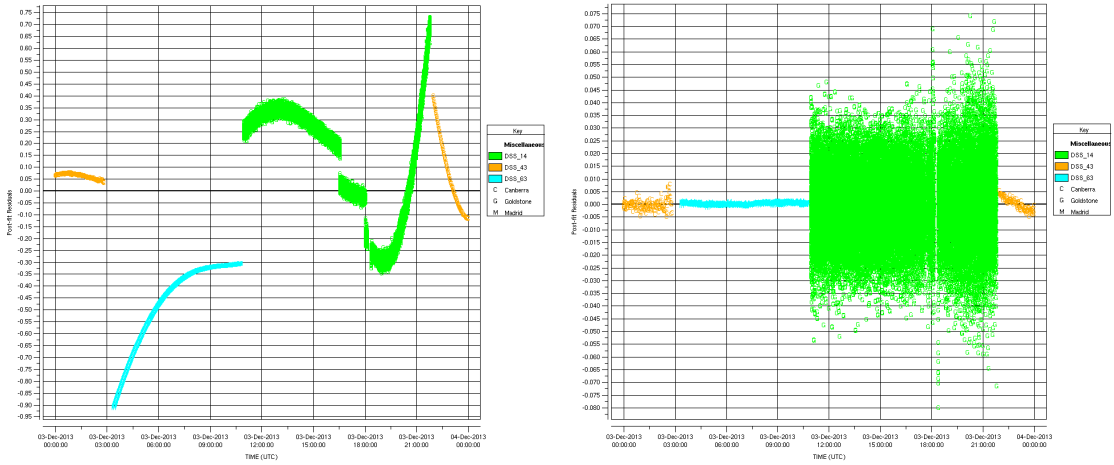

(a) Without IMU clock bias

(b) With 6-second IMU clock bias

Figure 5. MAVEN F2 Post-fit Residuals During TCM-1, with the use of IMU measurements.

radiometric data (two-way Doppler denoted F2 in what follows). An accelerometer bias was found empirically to be around 2.0×10^{-7} km/s^2, which was in agreement with the norm of the vector bias obtained from querying the bias directly (available as additional channelized telemetry data). The clock shift may be visualized by plotting the IMU residuals on the initial fit, over the duration of the burn. This is done in Fig. 4, with annotations to denote the start times of events as indicated by the

two data types. This result led to the realization that MAVEN carried a 6-second clock bias. This bias was used to adjust the accelerometer time tags as permitted via Eq. (1), and Figures 5(a)-5(a) illustrate the improved radiometric data fit that results.

Prior to TCM-2 the on-board clock was adjusted, in isolation of the plotted results. In fitting data over the TCM-2 burn, a reduced but non-zero 2-second clock bias is exhibited, shown in Fig. 6. The smaller magnitude clock bias had a negligible impact on the quality of the post-fit residuals, but this was at least in part a consequence of TCM-2 being a much smaller magnitude maneuver (relative to TCM-1). These calibration tests provide important information regarding clock and accelerometer magnitude biases, in preparation for the science phase. Moreover, the tests exercised tools specific to processing MAVEN telemetry, such as telemetry query and file parsing, and software for constructing raw torque and accelerometer measurements.

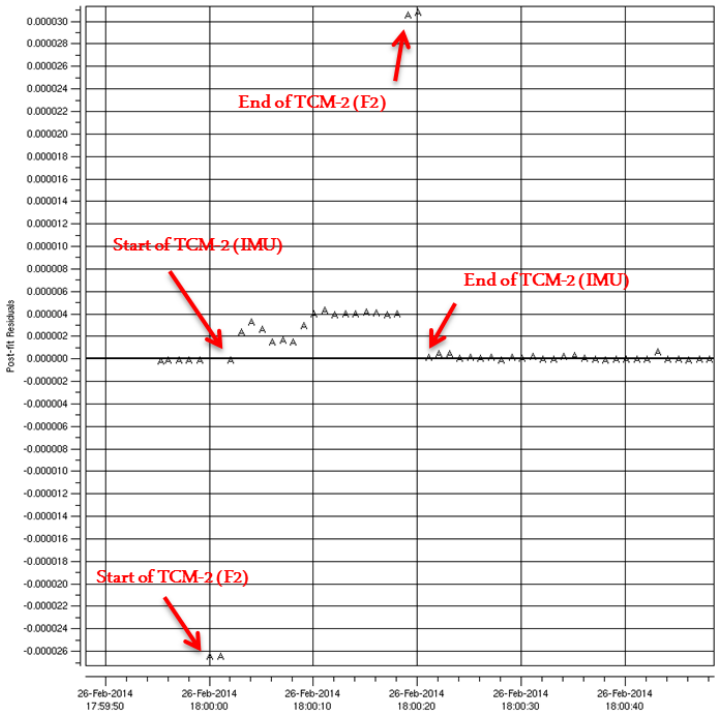

Figure 6. MAVEN Accelerometer Residuals during TCM-2, Annotated to Show Measurement Clock Offset.

Science phase testing using MRO IMU data

MRO IMU and radiometric data are used to test MAVEN developed setup and procedures, in preparation for nominal science phase. MRO aerobraking orbit no. 254 (08-AUG-2006 21:55:10 ET to 09-AUG-2006 05:34:00 ET), selected for this test, has periapsis (09-AUG-2006 01:58:55 ET) altitude of approximately 100 km. Figure 7 show postfit residuals (observed minus computed) for this test-case upon convergence, and Figure 8 a close-up of the IMU postfit residuals. The drag Δv for this periapsis passage is around 2.809 m/s. Although this is much higher than what MAVEN will experience during nominal science, it represents the best real-data test case for calibrations. For this test, the following parameters are estimated: state (position and velocity), solar pressure scale factor,

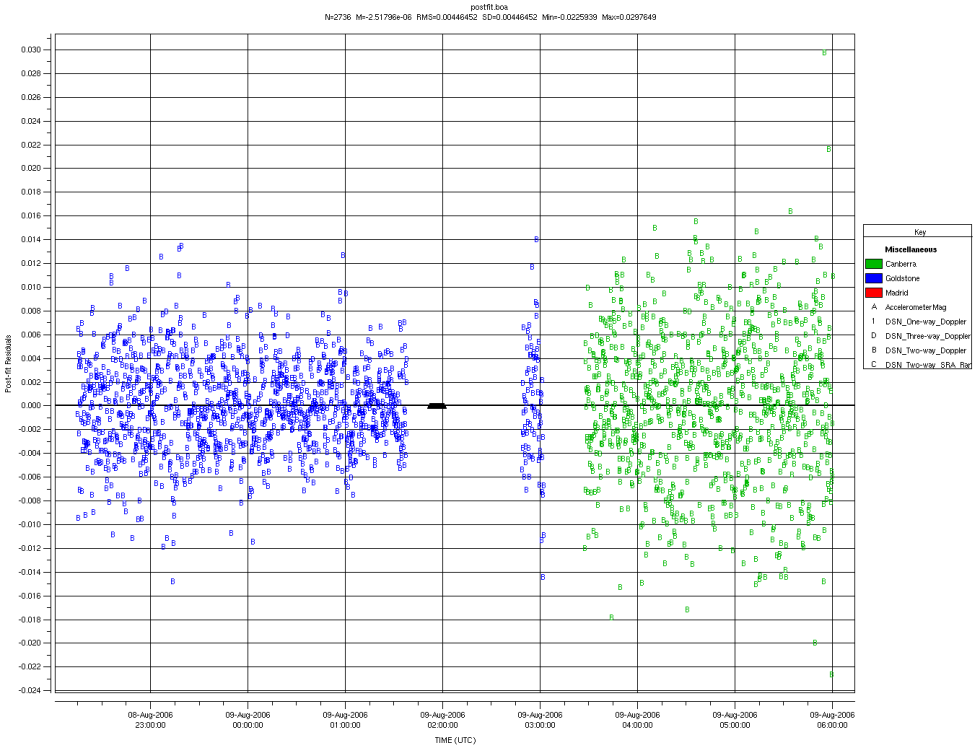

Figure 7. MRO Orbit 254 postfit residual (observed minus computed) plot: Two-Way (F2) Doppler and IMU data.

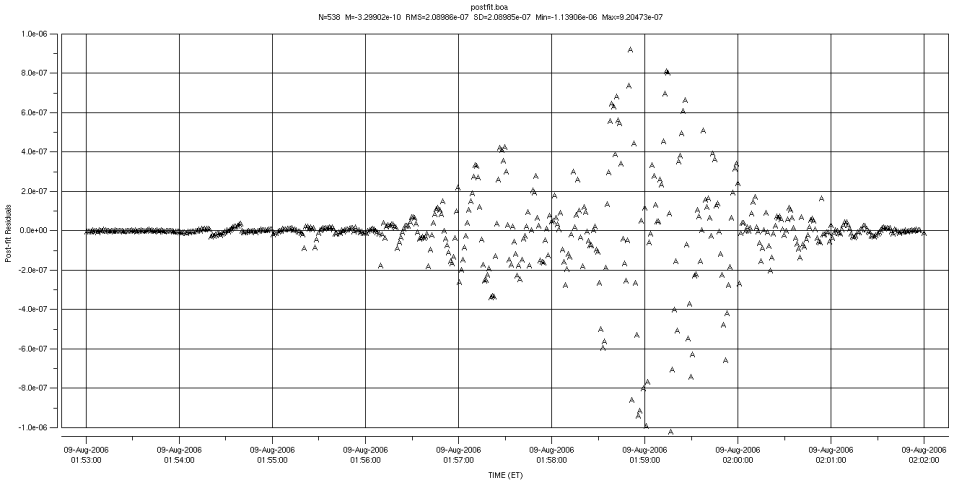

Figure 8. MRO Orbit 254 postfit residual (observed minus computed) plot: IMU data only.

density scale factor, and a polynomial acceleration (in three axes). The polynomial acceleration is used to account for errors in the atmospheric profile (smooth-out the residuals), where a simple scale factor cannot. Unlike MRO, doing this would cause problems for MAVEN (with its density corridor requirement), since the acceleration would tend to cause an under-estimation of the drag Δv, and thereby the density.

Maven science phase

Single Drag Pass Maven orbit no. 365 (periapsis 06-DEC-2014 22:42 ET), is considered as a representative nominal science phase prediction arc. Therefore, the arc covers a single tracking pass with a single drag pass. Figure 9 shows the accelerometer (IMU) observable, with a small peak for the drag pass (there is a data gap over the desat). The difficulty in utilizing this data, is that the drag acceleration magnitude is nearly on the order of the IMU noise (i.e. low signal to noise ratio). Figure 10 is a plot of drag acceleration from the observed and computed IMU observable, as well as from the scaled MG05 model (corrected using Doppler and IMU data). As annotated in the

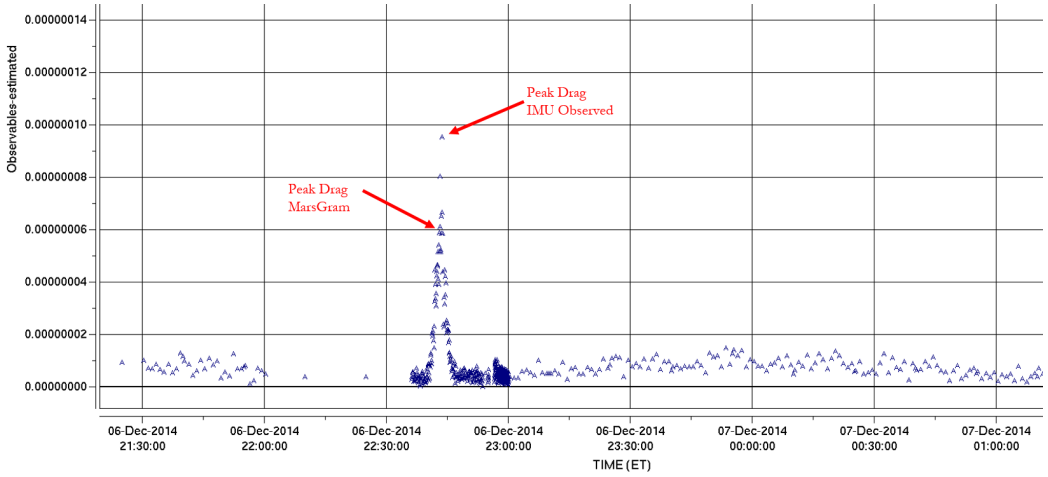

Figure 9. Maven Orbit 365 annotated IMU observables.

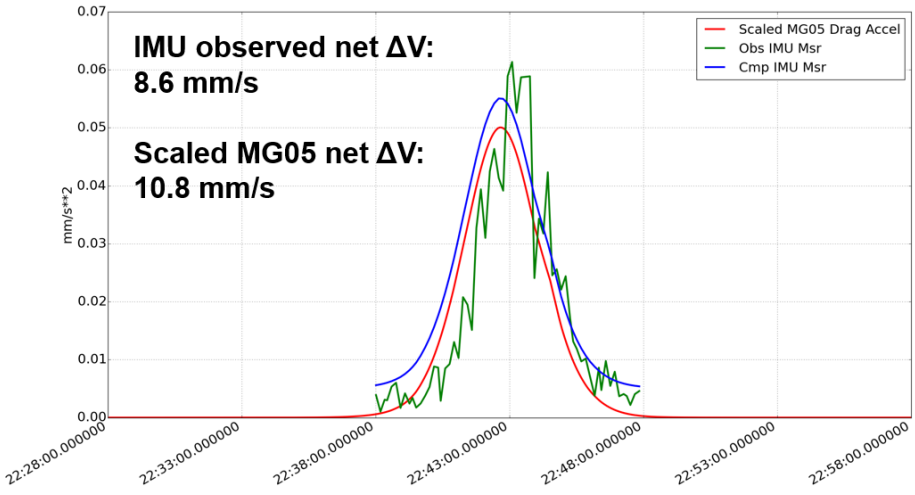

Figure 10. Maven Orbit 365 drag acceleration versus time

figures, the IMU shows the peak drag occurring around 30 seconds after the Mars-GRAM model; therefore suggesting a large transverse gradient. A shift was exhibited consistently to be between 10-60 seconds for multiple orbits, at high latitudes (> 50 degrees), and therefore likely represents a true (un-modeled in MG05) atmospheric phenomenon. Additionally, a small IMU bias of around

5.0×10^{-6} m/sec is apparent in Figures 9-10. The bias term b_a is set to this value, and not estimated further in what follows.

The orbit determination estimated parameters for this arc are: state (position and velocity), solar pressure scale factor, MG05 density scale factor (as stochastic), and an impulsive desat (in spacecraft body frame, about zero mean). The desat and solar pressure scale factor and estimated as constrained bias parameters. Table 1 summarizes the converged estimates (using both F2 and IMU data), for different IMU data weightings (state estimates exhibited negligible change and therefore those parameters are omitted). As indicated by Figure 10, the IMU suggests lower net drag Δv

Table 1. MAVEN Orbit 365 (Predict) Estimated Parameters using IMU and F2 data.

Parameter	IMU $\sigma = 2.0 \times 10^{-5}$ m/sec	IMU $\sigma = 5.0 \times 10^{-6}$ m/sec
SRP scale factor	1.010	1.084
MG05 density scale factor	0.339	0.326
Desat v_x, mm/sec	0.011	0.013
Desat v_y, mm/sec	-0.040	-0.257
Desat v_z, mm/sec	-0.002	-0.013

(area under the curve) than the Doppler data suggests, and therefore yields lower MG05 scale factor estimate. However, this may simply be an artifact of low signal-to-noise eliminating the Δv at the start and end of the drag pass. The loosely weighted IMU data, yields a solution which is nearly identical to a F2 data only solution. As more weight is given to the IMU, smaller density scale factor and larger desat acceleration result. However, there is very little helpful information for the desat and only marginally for the SRP scale factor (little reduction in parameter uncertainties), and since Mars-GRAM is only being scaled the shift in peak density epoch also does not alter the solution.

Reconstructed Batch of Orbits Orbit nos. 308-314 (Nov. 25-27, 2014) were selected as characteristic of a reconstruction batch. This batch consists of two tracking passes, with seven total drag passes, but only two are 'visible' in Doppler. Over this period MAVEN was Earth-pointed, and therefore the attitude (and effective drag area) is uniform. The motivation here is to use the IMU data to fill in the Doppler gap, in reconstructing the MG05 density scale factor stochastic estimates. This then provides additional (much needed) density information for science and for influencing prediction, which would otherwise have been lost. Figure 11 shows the converged F2 postfit residuals (with the large tracking gap), and Figure 12 the prefit IMU residuals over the arc (unconverged), with $b_a = 8.0 \times 10^{-9}$ m/sec.

Estimated parameters include: state, solar pressure scale factor (constrained), MG05 density scale factor (as stochastic), and impulsive desats (constrained in spacecraft body frame, about zero mean). Table 2 summarizes the converged estimates, versus IMU data weight (including F2 only). Again state estimates are omitted, and only the F2 observable desats are listed. In regions without Doppler data, impulsive maneuvers and density scale factor updates are essentially unobservable. Observability of orbit-to-orbit density (in the gap) is only available from the IMU data, although uncertainties are not reduced as much as those drag passes also having F2 data (on the order of 5.0×10^{-2} compared with 5.0×10^{-3}, respectively, and from an apriori of 0.2). The loose-weighted IMU solution is similar to the F2 only solution, but provides density estimates during the radiometric gap. Overall, the IMU data indicates the density during the arc was closer to that estimated for orbit

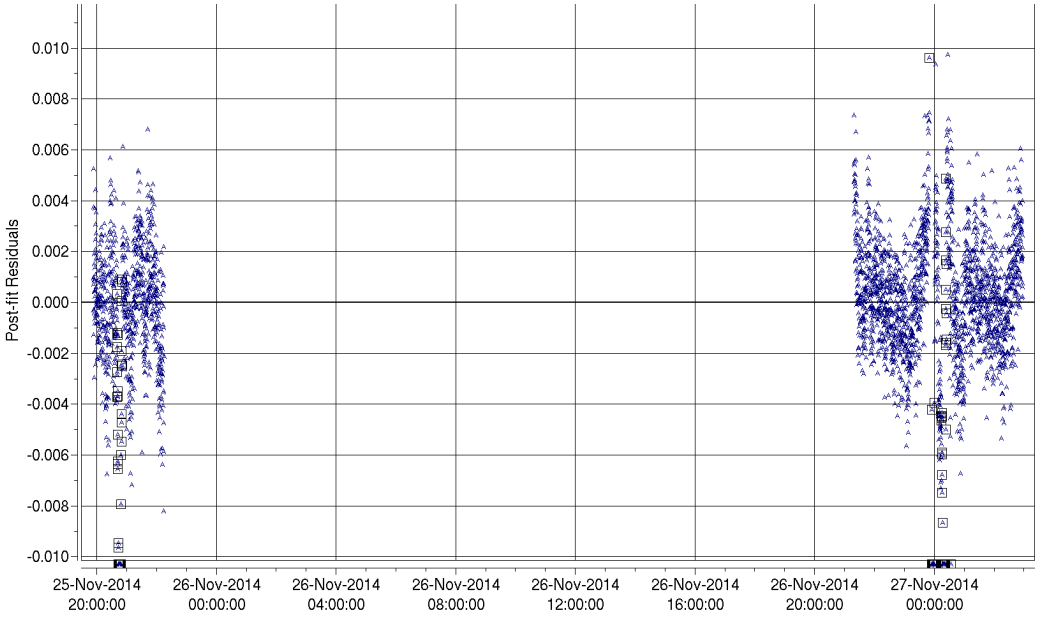

Figure 11. Maven Orbits 307-314 converged postfit F2 residuals.

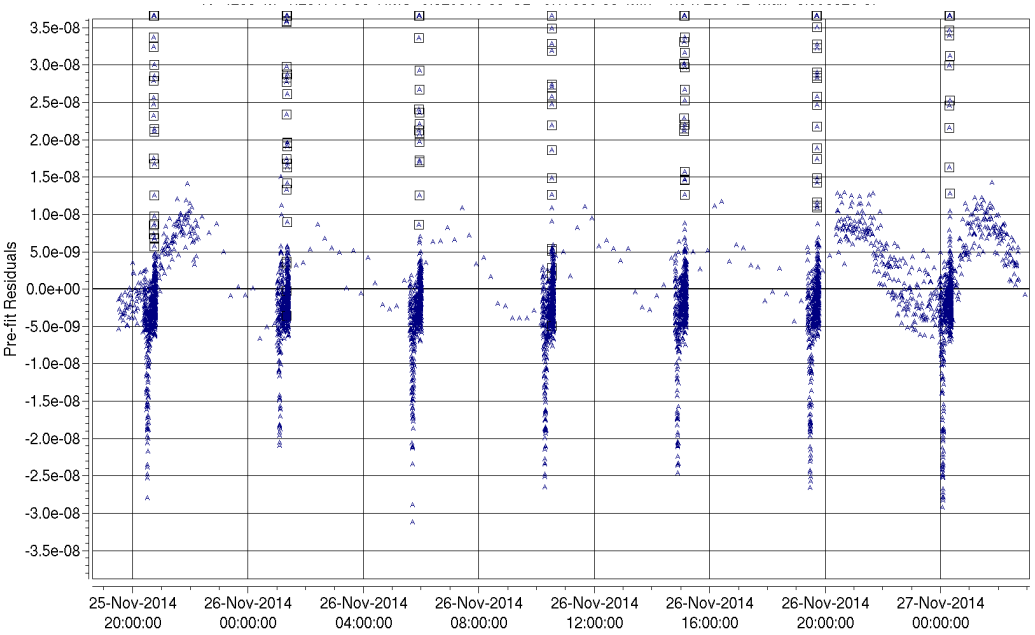

Figure 12. Maven Orbits 307-314 prefit IMU residuals.

no. 307 (higher), as opposed that of orbit no. 313. The mean MG05 scale factor varies from 0.407 (F2 only) to 0.441 (IMU $\sigma = 2.0 \times 10^{-5}$), and 0.426 for tightly-weighted IMU. This type of information is very important to MAVEN navigation (especially for Deep-Dip campaigns, and periods of large density dispersions).

Table 2. MAVEN Orbits 307-313 (Reconstruct) Estimated Parameters using IMU and F2 data.

Parameter	F2 only	IMU $\sigma = 2.0 \times 10^{-5}$ m/sec	IMU $\sigma = 5.0 \times 10^{-6}$ m/sec
SRP scale factor	0.897	0.896	0.879
MG05 density scale factor			
308	0.455	0.453	0.430
309	-	0.592	0.583
310	-	0.440	0.423
311	-	0.397	0.380
312	-	0.454	0.477
313	-	0.381	0.371
314	0.360	0.359	0.351
Desat v_x, mm/sec			
308	0.087	0.087	0.075
314	0.093	0.087	-0.001
Desat v_y, mm/sec			
308	0.011	-0.006	-0.207
314	0.070	0.062	-0.056
Desat v_z, mm/sec			
308	-0.039	-0.049	-0.178
314	-0.113	-0.118	-0.185

CONCLUSION

The successful demonstration of using telemetry data to improve the accuracy of ground based orbit determination could help to reduce cost (DSN tracking time) and increase performance of future NASA missions. In addition, it presents an important stepping stone to autonomous onboard aerobraking and aerocapture. The IMU accelerometer has proven a useful observable in supplementing MAVEN's limited tracking data, particularly for reconstructed density. However, the low signal-to-noise ratio at nominal science altitudes significantly reduces the power of the data type. Further effort is focused on reduce the noise, via smoothing and the implementation of a vector acceleration observable.

Also in future work, the torque observable as derived and described in this paper, will be used in the batch orbit determination process. The JPL MONTE software is currently being enhanced to support the necessary computations reliably enough for an operational mission. It is expected, that the more sensitive reaction wheel speed data and the vector observable will greatly enhance the effectiveness of this methodology.

ACKNOWLEDGMENTS

The authors would like to acknowledge and extend their gratitude to Stuart Demcak and Tung-Han You for their support and guidance. This work was carried out at the Jet Propulsion Laboratory, California Institute of Technology, under a contract with the National Aeronautics and Space Administration (NASA). Reference to any specific commercial product, process, or service by trade

REFERENCES

[1] S. Demcak, "Navigation Challenges in the Maven Science Phase," *23rd International Symposium on Space Flight Dynamics*, Pasadena, CA, 2012.

[2] G. Wawrzyniak and M. Lisano, "Using Inertial Measurements for the Reconstruction of 6-DOF Entry, Descent, and Landing Trajectory and Attitude Profiles," *AIAA/AAS Astrodynamics Specialists Conference*, 2002.

[3] R. Tolson, A. Dwyer, J. Hanna, G. Keating, B. George, P. Escalera, and M. Werner, "Application of accelerometer data to Mars Odyssey aerobraking and atmospheric modeling," *Journal of Spacecraft and Rockets*, Vol. 42, No. 3, 2005, pp. 435–443.

[4] M. K. Jah, M. E. Lisano, G. H. Born, and P. Axelrad, "Mars aerobraking spacecraft state estimation by processing inertial measurement unit data," *Journal of guidance, control, and dynamics*, Vol. 31, No. 6, 2008, pp. 1802–1812.

[5] D. J. O'Shaughnessy, D. J. Carrelli, J. T. Kaidy, T. E. Strikwerda, and H. Ambrose, "Autonomous Aerobraking Algorithm Testing in a Flight Software Simulation Environment," *dvances in the Astronautical Sciences*, Vol. 142, 2011.

[6] S. Flangan and T. Ely, "Navigation and mission analysis software for the next generation of JPL missions," *16th International Symposium on Space Flight Dynamics*, Pasadena, CA, 2001.

[7] C. G. Justus, "Aerocapture and Validation of Mars-GRAM with TES Data," *53rd JANNAF Propulsion Meeting and 2nd Liquid Propulsion Subcommitee and Spacecraft Propulsion Joint Meeting*, 2006.

[8] G. Bierman, *Factorization Methods for Discrete Sequential Estimation*, Vol. 128. Academic Press, 1977.

[9] M. Park and Y. Gao, "Error and Performance Analysis of MEMS-based Inertial Sensors with a Low-cost GPS Receiver," *Sensors*, No. 8, 2008, pp. 2240–2261.